Journal of Applied Polymer Science

Cotton Fibers Reinforcement of HNBR: Control of Fiber Alignment and Its Influence on Properties of HNBR Vulcanizates

Pimsaruta Sanprasert,[1] Narongrit Sombatsompop,[2] Pongdhorn Sae-oui,[3] Chakrit Sirisinha[1,4]

[1]Department of Chemistry, Faculty of Science, Mahidol University, Bangkok 10400, Thailand

[2]Polymer Processing and Flow (P-PROF) Group, School of Energy, Environment and Materials, King Mongkut's University of Technology Thonburi (KMUTT), Thung Khru, Bangmod, Bangkok 10140, Thailand

[3]National Metal and Materials Technology Center, 114 Thailand Science Park, Paholyothin Road, Klong 1, Klong-Luang, Pathumthani 12120, Thailand

[4]Rubber Technology Research Centre (RTEC), Faculty of Science, Mahidol University, Salaya Campus, Phutthamonthon 4 Rd., Salaya, Nakhon Pathom 73170, Thailand

Correspondence to: C. Sirisinha (E-mail: chakrit.sir@mahidol.ac.th)

ABSTRACT: This article focuses on the reinforcement of hydrogenated acrylonitrile butadiene rubber (HNBR) by cotton fiber as natural reinforcing filler. The effect of fiber alignment on the properties of HNBR compounds and vulcanizates is investigated. Properties of interest include rheological behavior, cure, tensile, abrasion, and dynamic mechanical properties which are correlated to the magnitudes of state-of-mix, bound rubber content, crosslink density and fiber alignment. Results obtained reveal that mechanical properties of rubber composites are improved dramatically by the addition of cotton fiber due to the enhanced hydrodynamic effect in association with crosslink density. Furthermore, the degree of fiber alignment is found to depend strongly on shear strain. The results demonstrate the importance of fiber alignment controlled efficiently by shear strain. © 2014 Wiley Periodicals, Inc. J. Appl. Polym. Sci. **2014**, *131*, 41090.

KEYWORDS: composites; elastomers; properties and characterization; rubber

Received 27 November 2013; accepted 27 May 2014
DOI: 10.1002/app.41090

INTRODUCTION

Typically, reinforcement of rubber vulcanizates has widely been conducted by the use of aggregate reinforcing fillers, such as carbon black and silica. However, a high loading of reinforcing filler is often required to achieve desirable degree of reinforcement which in turn causes processing difficulty, that is, poor filler dispersion and excessive bulk viscosity. One possible solution is the replacement of aggregate fillers with fibrillar fillers having high aspect ratio. Such fillers include aramid fiber, fibrillar silicate, silk, and cellulose fibers.[1–5]

Short fiber reinforced rubber composites (SFRCs) are mostly known nowadays because they possess good mechanical properties such as modulus and strength even at low fiber loading. Generally, there are many factors controlling reinforcing efficiency of short-fiber, that is, fiber aspect ratio, orientation, dispersion degree and rubber–fiber adhesion.[1–4,6] It has been reported that fiber alignment plays substantial role in anisotropy of reinforcement efficiency in SFRCs.[3,7] In most cases, the SFRCs possess higher mechanical strength than the composites reinforced with particulate fillers such as carbon black.[8] Typically, surfaces of most natural fibers are rough, enhancing the interfacial adhesion between polymer matrix and fiber surfaces via mechanical interlocking mechanism.[9] Cotton fiber is one of the most widely used natural reinforcing fibers due to its high strength and modulus. Also, the cotton fiber is classified as green and renewable material. This makes the cotton fiber advantageous in ecological and environmental friendliness. However, due to regular arrangement of the cellulosic structure, the cotton fiber tends to form tight agglomerates via hydrogen bond making it more difficult to be dispersed throughout the rubber matrix. Thus, the approach to achieve good fiber dispersion with controllable fiber alignment is challenging. Referring to previous studies on SFRCs, bonding agents could significantly improve an interfacial adhesion between fibers and rubber matrix. For example, in nitrile rubber (NBR) reinforced with silk fiber, the use of a resorcinol-hexamethylenetetramine-silica as a bonding agent is found to augment mechanical properties of the composites.[4] It must be noted that the optimal amount of bonding agent is required. Excessive loading of

Table I. Compounding Recipe Used in this Work

Ingredients	Amount (phr)	Function
HNBR	100	Raw rubber
Cotton fiber	0, 5, 10, 15	Reinforcing filler
Stearic acid	0.5	Softener
Luperox F40P SP2	6.25	Curing agent
TAIC	2.5	Co-agent

bonding agents could give detrimental effect on mechanical properties of composites.[10] Although there are some reports on SFRCs,[2–4,6,7,11–14] the number of published work focusing on hydrogenated nitrile rubber (HNBR) reinforced with cotton fiber is still limited. In general, the fiber-reinforced HNBR composites are of interest in numerous engineering products requiring high mechanical strength under high-temperature hydrocarbon oil environment. These include industrial rollers in which high mechanical strength with low heat buildup are desired. In the present work, cotton fiber was used as reinforcing filler for HNBR in order to enhance mechanical properties while maintaining its environmental-friendliness. This work therefore focused on approaches to achieve good fiber dispersion and controllable fiber alignment. Additionally, influence of cotton fiber content on viscoelastic behavior and mechanical properties of HNBR composites was investigated.

EXPERIMENTAL

Materials

HNBR (Zetpol 2030 L; acrylonitrile content = 36%; residual double bond = 15%) was manufactured by Zeon Chemicals (Japan). Cotton fiber (LM-5) with average diameter, length and L/D ratio of 0.014 mm, 0.45 mm, and L/D = 32, respectively, was pre-treated with resorcinol formaldehyde latex (RFL) by Heilongjiang Hongyu Novel Short Fiber Materials Co., Ltd. (China). Stearic acid was supplied from Chemmin Co., Ltd. (Thailand). 1,3-1,4-Bis(tert-butylperoxyisopropyl) benzene (Luperox F40P-SP2) as curative and Triallyl isocyanurate (TAIC) as co-agent were supplied by Arkema (Thailand) and Chemmin Co., Ltd. (Thailand), respectively. Methyl ethyl ketone (MEK) was purchased from V.S. Chem House (Thailand).

Rubber Composite Preparation

Table I represents the compounding recipes used in this work. The formulation containing 15% of cotton fibers was chosen for the "state-of-mix" study. Prior to being used, the cotton fiber was de-humidified in hot-air oven at 80°C for 24 hours. For fiber alignment study, mixing was conducted using two-roll mill with three mixing steps. In the 1st step, HNBR was masticated and followed by the addition of cotton fiber. Shear stress was varied by changing nip width (0.2, 0.4, and 0.6 mm) while mixing times were varied from 8 to 12 minutes. The mix was then discharged and cooled down. Peroxide and TAIC were then incorporated in the 2nd step. After mixing for 10 minutes, the mix was again cooled down to room temperature. The 3rd step was intended to control the shear strain applied to the mix. The mix from the 2nd step was passed through the narrow nip width of 0.02 mm. The number of passage was varied from 6 to 15 to alter magnitude of shear strain. The shear strain applied to polymer in the nip region in each passage (designated as SP) was indirectly calculated from shear strain rate ($\dot{\gamma}$) as illustrated in eqs. (1–3):

$$\dot{\gamma} = \frac{d\gamma}{dt} = \frac{v}{h} \tag{1}$$

$$\mathrm{SP} = \dot{\gamma} \times t \tag{2}$$

$$\mathrm{SP} = \dot{\gamma} \times t = \frac{(v_1 - v_2)}{h} \times t = 2.0 \times 10^3 t \tag{3}$$

where t is duration of the rubber compound residing in the nip region; v_1 and v_2 are velocities of back and front rolls [i.e., 0.214 m/s (27 rpm) and 0.175 m/s (22 rpm)], respectively; h is the nip width. According to eq. (1), the calculated shear rate is based on the difference in velocities of front and back rolls. Two assumptions are applied as follows: (i) flow in the nip region is steady shear flow and (ii) the residence time (t) in the nip region is constant. As calculated from eqs. (2) and (3), the arbitrary value of strain applied to rubber in the nip region in each passage (SP) is 2.0×10^3 t. By varying the number of passage, the calculated strain is varied as follows: 1.2×10^4t, 1.8×10^4t, 2.4×10^4t and 3.0×10^4t. For fiber loading study, mixing was also carried out on two-roll mill using the three mixing step as previously described. However, in this part, the nip width and mixing time of the 1st step was fixed at 0.2 mm and 10 minutes, respectively, and the number of passage in the 3rd step was fixed at 15 (3.0×10^4t).

Curing of rubber compounds was conducted using a hydraulic hot-press at 170°C under clamping pressure of 15 MPa with reference to the cure time pre-determined from the oscillating disc rheometer (ODR; Monsanto R-100).

Characterization of Rubber Compounds

Cure characteristics of cotton-filled HNBR were measured using the oscillating disc rheometer (ODR; Monsanto R-100). Optimal cure time (t_c95) was determined from the time to reach 95% cure state. Torque difference (M_H–M_L) between the maximum (M_H) and minimum (M_L) storage torques was considered as an indication of crosslink density.[15–17]

Bound rubber content is a measure of interaction magnitude between filler and rubber matrix. Small pieces of rubber compounds were immersed in MEK (as good solvent for HNBR) for 7 days at room temperature to achieve full extraction of soluble rubber portion. Then, an insoluble portion was filtered and dried at 80°C for 2 hours. The bound rubber content was calculated using eq. (4):[18]

$$R_b(\%) = 100 \times \frac{[W_{fg} - W_t(m_f/(m_f + m_r)]}{W_t(m_f/(m_f + m_r)} \tag{4}$$

where R_b is bound rubber content; W_{fg} is weight of fiber and gel; W_t is weight of specimen; m_f and m_r are weights of fiber and rubber in compound, respectively.

Rheological Study

Rheological study was conducted in both rubber compounds and vulcanizates. For the rubber compounds, Mooney viscosity was measured under steady shear flow at 100°C using Mooney viscometer (VisTECH+, TechPro). For the vulcanizates,

rheological behavior was studied under oscillatory flow using a Rubber Process Analyzer (RPA2000; Alpha Technologies). The compounds were first cured in RPA2000 cavity at 170°C and, then, the die temperature was decreased to 100°C for performing the strain sweep test (i.e., strain range of 0.5–100.02%) at a given angular frequency of 2 rad/s. Storage modulus (G′) of the vulcanizates was recorded, and the discrepancy in G′ at strains of 2 and 100% was taken as a magnitude of Payne effect (ΔG′). The lower magnitude of ΔG′ suggests the lower degree of filler network, and thus the greater degree of filler dispersion.[19,20] In addition to RPA2000, a dynamic mechanical analyzer (Gabo, Explexor 25N, Germany) was utilized to determine the viscoelastic properties of HNBR vulcanizates under tension mode with static and dynamic strain amplitudes of 2 and 0.1%, respectively. Temperature sweep test was performed from −80 to 70°C with a scanning rate of 2°C/min and a test frequency of 10 Hz.

Morphological Observation

Fiber dispersion and alignment were characterized qualitatively by the use of light microscope (VZM-1510; Itokin Technology Co., Japan). Surfaces of cured sheets with thickness of approximately 1 mm were cleaned to remove dusts before viewing. Apart from light microscope, a scanning electron microscope (JSM6400; JEOL Ltd., Japan) was utilized to study the mechanical failure behavior. Fractured surfaces of rubber specimens from the tensile test were sputtered with gold before observation.

Mechanical Properties

Tensile properties were measured according to ASTM D412 while tear strength was measured as per ASTM D624. To investigate the effect of fiber alignment, the tests were performed in both longitudinal (L) and transverse (T) directions using a universal mechanical tester (Instron 5569) at a crosshead speed of 500 mm/min with a load cell of 1 kN. Hardness was determined on the cured specimens with thickness of at least 6 mm by the use of Shore A durometer (Wallace H17A, UK) at room temperature according to ASTM D2240-97.

Crosslink Density

In addition to the torque difference (M_H–M_L), crosslink density as defined by a number of active network chains per volume unit was determined by a swelling test via Flory-Rehner equation as illustrated in eq. (5). The specimens were weighed and then immersed in an excess of MEK at room temperature. After 7 days of swelling, the swollen specimens were weighed, and the elastically active network chains density (V_e) or crosslink density was calculated:

$$V_e = -\frac{\ln(1-V_r)+V_r+\chi V_r^2}{V_s\left(V_r^{1/3}-V_r/2\right)} \quad (5)$$

$$V_r = \frac{m_0\phi\left(\frac{1-\alpha}{\rho_r}\right)}{m_0\phi\left(\frac{1-\alpha}{\rho_r}\right)+\frac{m_1-m_2}{\rho_s}} \quad (6)$$

where V_r is the volume fraction of rubber in the swollen vulcanizate calculated from eq. (6); m_0 is the specimen mass before swelling; m_1 and m_2 are specimen masses before and after drying, respectively; Ø is the mass fraction of rubber in the composites; α is the mass loss of the gum HNBR vulcanizate during the swelling process; ρ_r and ρ_s are densities of rubber and solvent, respectively; χ is the polymer–solvent interaction parameter (0.453 for HNBR-MEK) and V_s is the solvent molar volume (90.2 cm^3/mol for MEK)[21,22]

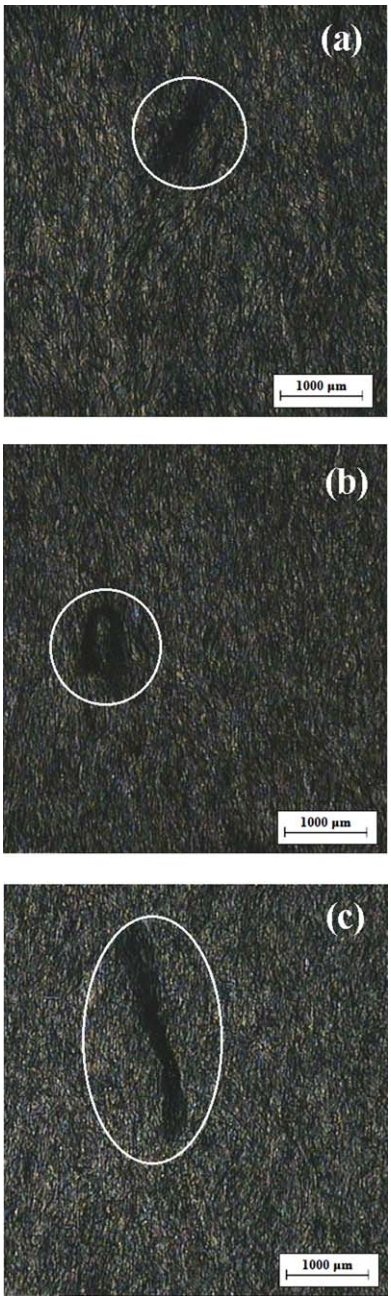

Figure 1. Micrographs (13x) of fiber-filled HNBR vulcanizates prepared with various nip widths: (a) 0.2 mm; (b) 0.4 mm; and (c) 0.6 mm. [Color figure can be viewed in the online issue, which is available at wileyonlinelibrary.com.]

RESULTS AND DISCUSSION

Effect of State-of-Mix

Figure 1 reveals optical micrographs of fiber-filled HNBR vulcanizates prepared with various magnitude of shear stress via

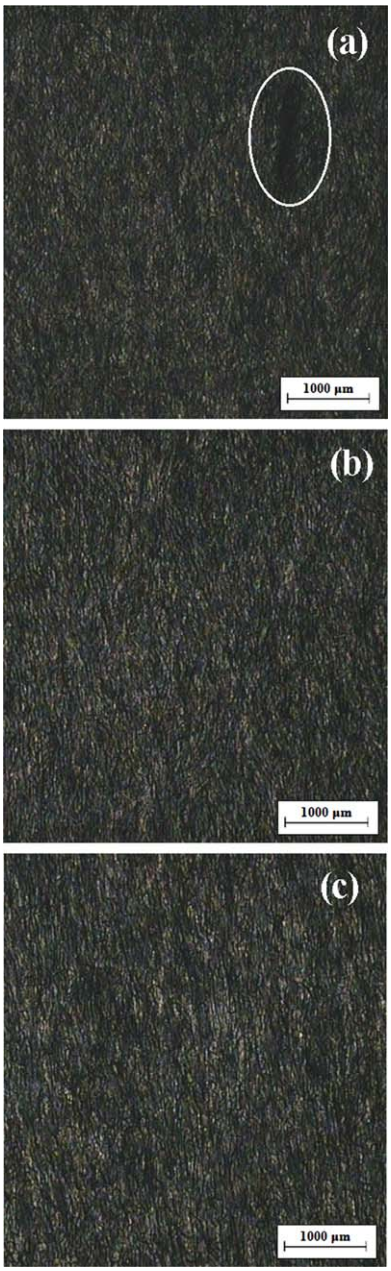

Figure 2. Micrographs (13x) of fiber-filled HNBR vulcanizates prepared with various mixing times: (a) 8 mins.; (b) 10 mins.; and (c) 12 mins. [Color figure can be viewed in the online issue, which is available at wileyonlinelibrary.com.]

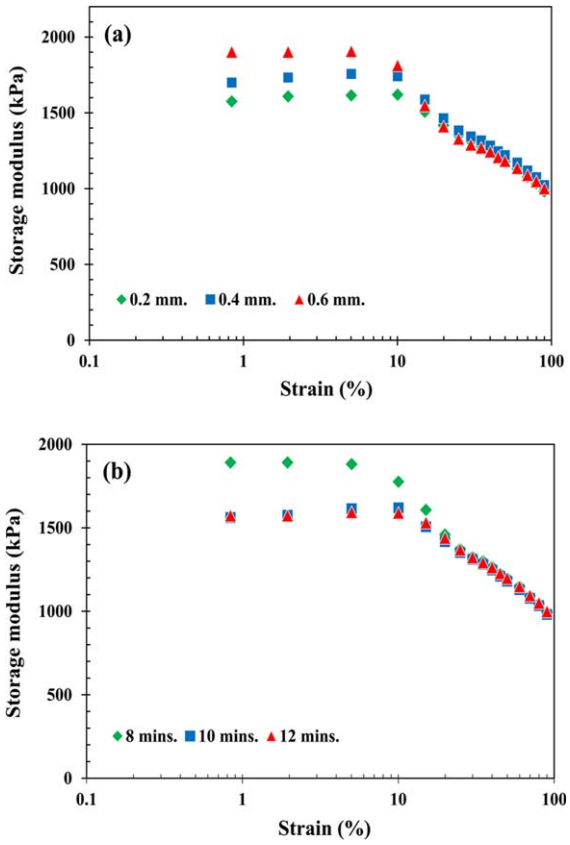

Figure 3. Storage modulus (G′) as a function of shear strain of fiber-filled HNBR vulcanizates prepared with different mixing parameters: (a) nip widths; (b) mixing times. [Color figure can be viewed in the online issue, which is available at wileyonlinelibrary.com.]

nip width adjustment. At large nip widths (0.4 and 0.6 mm), large agglomerates of cotton fibers are observed indicating poor degree of fiber dispersion. However, by decreasing the nip width to 0.2 mm, agglomerate size is reduced significantly, suggesting the drastic improvement in degree of fiber dispersion. Such improvement is explained by the increased shear stress and/or strain applied to the rubber, as illustrated in eq. (1).

Figure 2 demonstrates optical micrographs of vulcanizates mixed with various mixing times. Evidently, an increase in mixing time from 8 to 10 minutes leads to obvious enhancement in fiber dispersion. Such improvement in state-of-mix is due to the increase in magnitude of shear stress/strain applied to the rubber bulk. However, further increase in mixing time gives no significant change in degree of fiber dispersion. With prolonged mixing time, the shear heating caused by viscous dissipation gives rise to the increase in bulk temperature during the mixing process, which in turn reduces the shear stress applied to the rubber bulk. Simultaneously, when the filler size decreases, the critical stress required for breaking up the filler (also known as yield stress) increases. These lead to the unchanged state-of-mix as the mixing time is increased from 10 to 12 mins.

Figure 3 exhibits the strain sweep test results of HNBR systems with different nip widths and mixing times. With decreasing nip width, shear storage modulus (G′) at low strain reduces. This is also true for the increase in mixing time. Such high G′ at low strain is caused by a large amount of filler network containing immobilized rubber acting as parts of undeformable filler. With increasing shear strain, the disruption of filler network causes a release of immobilized rubber to become mobilized rubber as evidenced by a decrease in G′ at high strain. Table II reports physical characteristics and mechanical properties of fiber-filled HNBR vulcanizates with different milling conditions. The difference in G′ at low and high strains (ΔG′) or the so-called Payne effect is tabulated. From the results, ΔG′ appears

Table II. Properties of Fiber-filled HNBR Composites in the Study of State-of-Mix

	Fiber	Nip width (mm)			Mixing time (min)		
Property	Orientation	0.2	0.4	0.6	8	10	12
Payne effect (ΔG′) (kPa)	-	643 ± 58	720 ± 80	941 ± 101	940 ± 106	630 ± 97	619 ± 88
Hardness (Shore A)	-	70 ± 1	71 ± 1	71 ± 2	72 ± 2	72 ± 2	72 ± 2
Tensile strength (MPa)	L	5.1 ± 0.5	4.7 ± 0.3	4.6 ± 0.2	4.7 ± 0.2	5.2 ± 0.1	5.2 ± 0.2
	T	2.7 ± 0.1	2.6 ± 0.3	2.5 ± 0.3	3.0 ± 0.3	3.1 ± 0.1	3.1 ± 0.0
Elongation at break (%)	L	27 ± 4	20 ± 1	20 ± 5	23 ± 2	31 ± 3	34 ± 7
	T	189 ± 32	141 ± 14	137 ± 21	133 ± 8	193 ± 30	199 ± 11
25% Modulus (M25) (MPa)	L	4.9 ± 0.1	N/A[a]	N/A[a]	N/A[a]	5.1 ± 0.1	4.9 ± 0.4
	T	1.7 ± 0.2	1.3 ± 0.2	1.6 ± 0.2	1.0 ± 0.1	2.0 ± 0.2	1.3 ± 0.1
Tear strength (kN/m)	L	33.6 ± 0.6	31.0 ± 1.2	30.8 ± 1.4	33.7 ± 2.4	34.1 ± 0.3	36.8 ± 2.7
	T	27.8 ± 1.4	21.1 ± 0.4	20.2 ± 1.1	30.8 ± 1.8	± 0.3	35.2 ± 2.2

[a] M25 could not be determined due to the elongation at break lower than 25%.

to decrease with decreasing nip width or increasing mixing time. This suggests the enhancement in filler dispersion supporting the morphological results as discussed previously. With increasing state-of-mix via reduced nip width and/or increased mixing time, the improvement in tensile properties is resulted. Tensile strength and elongation at break are increased due to a reduction in the number of fiber agglomerates acting as flaws in the rubber matrix. This is also true for the tear strength. Noticeably, there is a strong anisotropic effect of cotton fiber on the vulcanizates as influenced by mixing conditions. In L direction, tensile strength, modulus and tear strength are greater whereas the elongation at break is lower, compared to those in T direction.

Regarding the degree of fiber alignment, Figure 4 shows the micrographs of vulcanizates prepared with optimal nip width and mixing time (i.e., 0.2 mm and 10 mins.). The vulcanizates were prepared with different numbers of passage (i.e., shear strains were varied from 1.2×10^4t to 3.0×10^4t. Evidently, good fiber dispersion in association with high magnitude of fiber alignment is observed when the rubber is subjected to high shear strain (3.0×10^4t) during the mixing process. In other words, the increase in shear strain magnitude applied to rubber matrix is capable of enhancing the fiber alignment along the shear field direction.

In order to determine the magnitude of anisotropy, ratios of mechanical properties in L direction to those in T direction are calculated, and then plotted as a function of shear strain imposed to the rubber bulk (Figure 5). Obviously, fiber alignment in L direction is more pronounced with increasing shear strain due to greater viscoelastic deformation of HNBR matrix. This leads to the increased reinforcement magnitude in the L direction, and thus the ratio of properties in L to T directions.

Effect of Fiber Loading

Table III shows physical characteristics and mechanical properties of HNBR compounds filled with various loadings of cotton fiber. With increasing cotton fiber loading, Mooney viscosity significantly increases which is attributed to the hydrodynamic effect in association with a formation of immobilized rubber in fiber network and/or agglomerates. This suggests a decrease in processability with increased fiber loading. One might expect that such increase in viscosity is also due to the increase in rubber–filler interaction. As evidenced in the bound rubber results given in Table III, the bound rubber content is rather low even

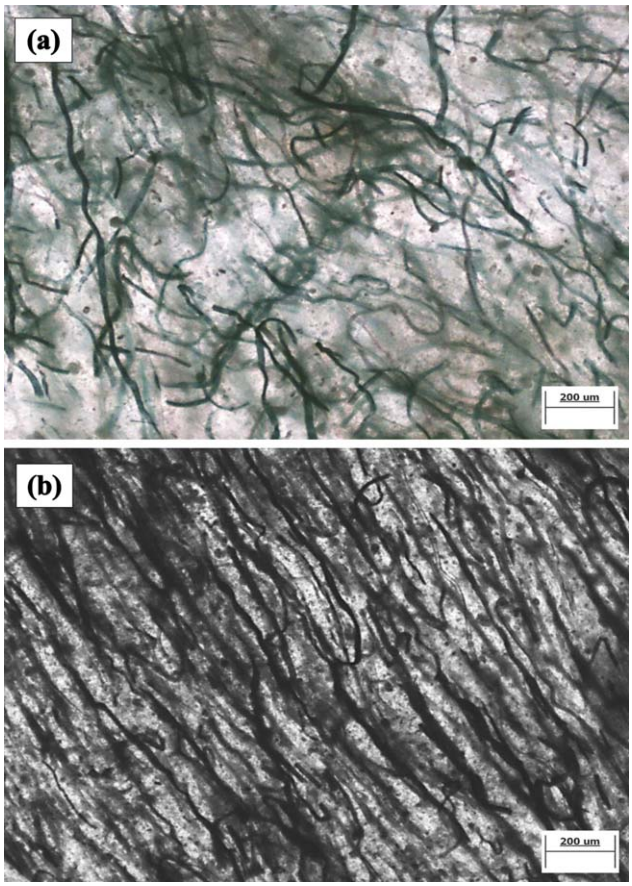

Figure 4. Micrographs (50x) of fiber-filled HNBR vulcanizates prepared with various shear strains: (a) 1.2×10^4t; (b) 3.0×10^4t. [Color figure can be viewed in the online issue, which is available at wileyonlinelibrary.com.]

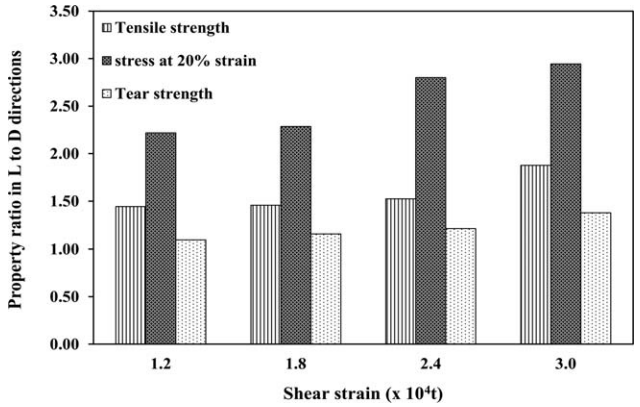

Figure 5. Anisotropic effects of fiber-filled HNBR vulcanizates as a function of shear strain.

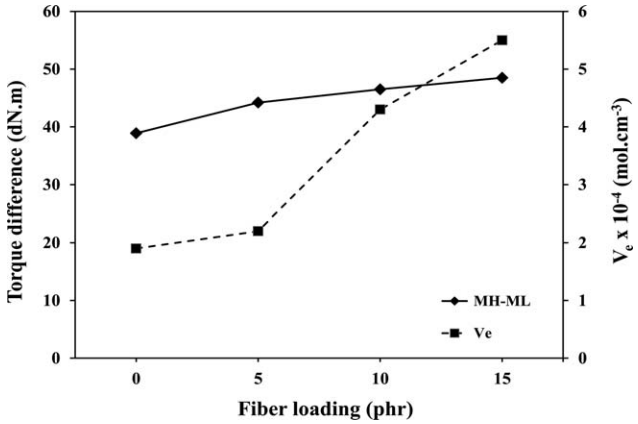

Figure 6. Crosslink density of HNBR composites with various fiber loadings.

at high fiber loading of 15 phr. This finding is much different from that found in the systems filled with particulate reinforcing fillers including carbon black and precipitated silica.[23,24] In other words, the influence of rubber–polymer interaction on Mooney viscosity could be disregarded in this work.

Apart from Mooney viscosity, cure characteristics of HNBR compounds change significantly with increasing fiber loading. A decrease in optimum cure time is observed, which is in good accordance with a rise in crosslink density of HNBR vulcanizates as determined from torque difference and swelling test via the Flory–Rehner equation as shown in Figure 6. The explanation of a cure promotion phenomenon found with increasing fiber loading is proposed in the aspect of thermal history during the mixing process. It is known that when filler loading increases, an increase in bulk viscosity leads to the increased shear heating and thus the accelerated rate of vulcanization.[25]

Regarding the magnitude of filler–rubber interaction influenced by cotton fiber loading, the results (Table III) exhibit relatively low bound rubber content (BRC) compared to those of the carbon black-filled nitrile rubber.[23,24] Anyway, there is still a trend of slight increase in BRC with fiber loading. The increase in contact surface area due to the increase in fiber loading is believed to be responsible for such slight increase in BRC.

Table III and Figure 7 reveal hardness and modulus results in which the increases in both are observed with increasing fiber loading. Such increases are caused by a combined effect of hydrodynamic effect, rubber–filler interaction and filler–filler interaction. Similarity in result trends of hardness and modulus at low strain is not unusual because it is widely known that the measurement of hardness is analogous to the measurement of modulus at specimen surface.[10,26] Furthermore, at a given fiber loading, the modulus in L direction is greater than that in T direction. This is more pronounced in the case of low strain where a large amount of filler network exists. This finding is also applicable to tensile strength and elongation at break. It seems that the cotton fiber helps increasing load-bearing capability of test specimens. The alignment of fiber in the L direction (parallel to the applied load) could distribute the load more effectively than that in the T direction. On the other hand, the elongation at break decreases with increasing fiber loading particularly in the L direction. Referring to the modulus results illustrated previously in Figure 7, the modulus increases

Table III. Physical Characteristics and Mechanical Properties of HNBR Compounds in the Study of Effect of Fiber Loading

	Fiber	Fiber loading (phr)			
Property	Orientation	0	5	10	15
Scorch time (t_s2) (min)	–	2.3 ± 0.2	2.3 ± 0.0	2.3 ± 0.1	2.3 ± 0.0
Optimum cure time (t_c95) (min)	–	20.4 ± 0.1	19.2 ± 0.1	18.4 ± 0.2	18.1 ± 0.0
Mooney viscosity (MU)	–	36.4 ± 0.5	39.1 ± 0.9	44.2 ± 0.4	49.2 ± 1.1
Bound rubber (%)	–	2.4 ± 0.1	2.7 ± 0.2	3.8 ± 0.5	3.9 ± 0.3
Hardness (Shore A)	–	50 ± 1	60 ± 1	66 ± 1	72 ± 1
Tensile strength (MPa)	L	2.7 ± 0.4	2.7 ± 0.1	3.4 ± 0.5	4.7 ±0.3
	T	–	2.1 ± 0.1	2.3 ± 0.1	2.5 ± 0.1
Elongation at break (%)	L	280 ± 7	72 ± 16	51 ± 23	20 ± 8
	T	–	179 ± 12	169 ± 25	158 ± 20
Tear strength (kN/m)	L	11.7 ± 0.6	20.6 ± 2.5	24.8 ± 1.5	33.0 ± 1.2
	T	–	17.8 ± 1.0	23.1 ± 1.2	26.4 ± 0.8

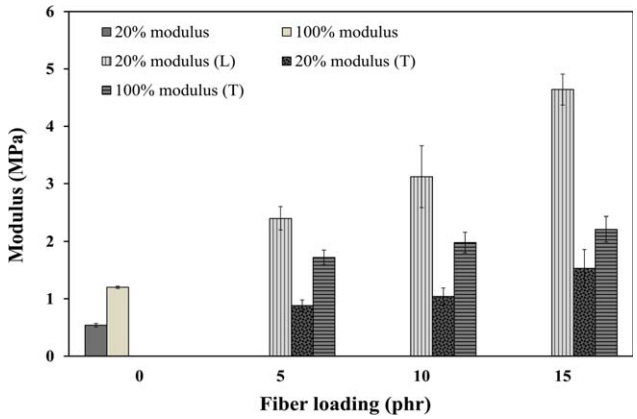

Figure 7. Modulus of HNBR composites with various fiber loadings. [Color figure can be viewed in the online issue, which is available at wileyonlinelibrary.com.]

with increasing fiber loading, particularly in the L direction. Thus, the relatively high modulus and strength of fiber (compared with HNBR matrix) restricts the bulk deformation.

Tear strength is found to increase with the increase in fiber loading, especially in the L direction. The results agree well with the tensile strength and modulus. Such enhancement in tear strength by fiber addition is explained not only by load-bearing capability of fiber but also by the energy dissipation as a result of zig–zag route formation.[27]

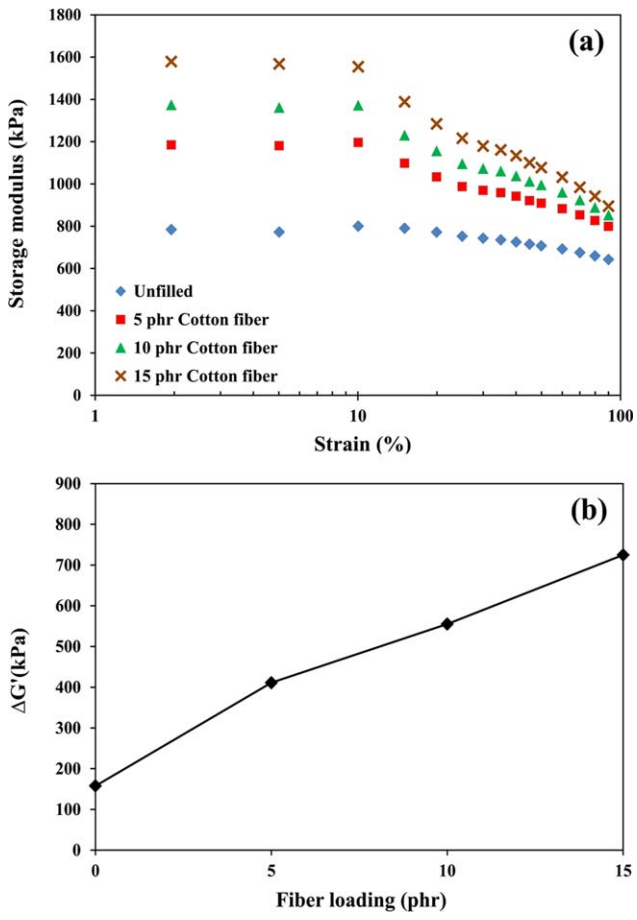

Figure 8. Strain sweep test results of HNBR composites with various fiber loadings: (a) storage modulus (G′); (b) magnitude of Payne effects (ΔG′). [Color figure can be viewed in the online issue, which is available at wileyonlinelibrary.com.]

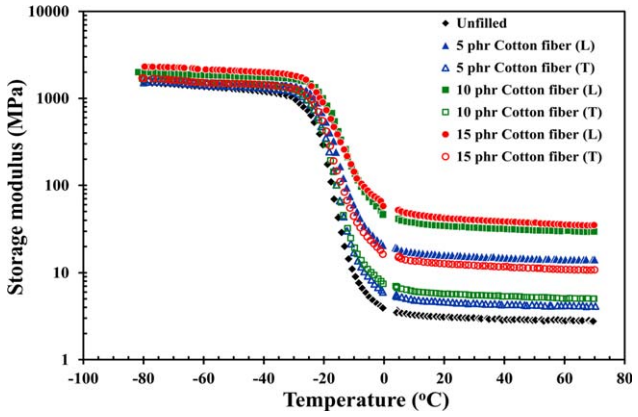

Figure 9. Effect of fiber loading on storage modulus (E′) of HNBR composites with various fiber loadings. [Color figure can be viewed in the online issue, which is available at wileyonlinelibrary.com.]

Figure 8(a) demonstrates strain sweep test results of HNBR vulcanizates with various cotton fiber loadings. Evidently, the G′ at low strain significantly increases with increasing fiber loading. This suggests the increase in hydrodynamic effect in association with increased magnitude of filler network formation.[19] With increasing strain, the G′ of all systems decreases, and the greatest change in G′ is observed in the system with the highest fiber loading. Such reduction in G′ indicates the non-linearity of G′ as a result of filler network disruption. Since the filler network is caused by the H-bond between hydroxyl groups on cellulosic fiber surfaces, the network is transient and can be broken down at high strain. By considering the magnitude of Payne effect (ΔG′) as shown in Figure 8(b), the ΔG′ increases progressively with fiber loading, supporting the explanation of filler network formation as discussed previously.

Figures. 9 and 10 reveal the temperature sweep test results. Referring to Figure 9, a drastic change in tensile storage

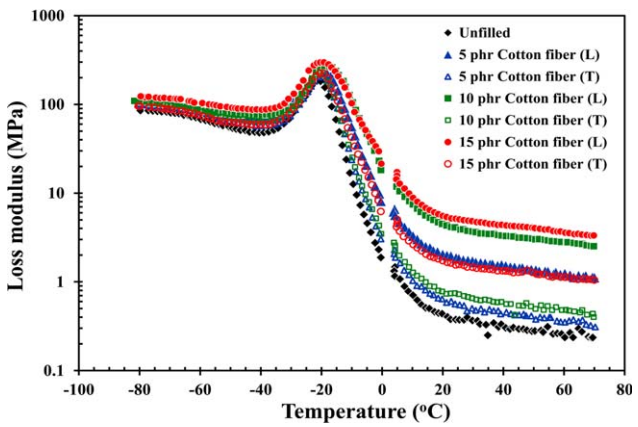

Figure 10. Effect of fiber loading on loss modulus (E") of HNBR composites with various fiber loadings. [Color figure can be viewed in the online issue, which is available at wileyonlinelibrary.com.]

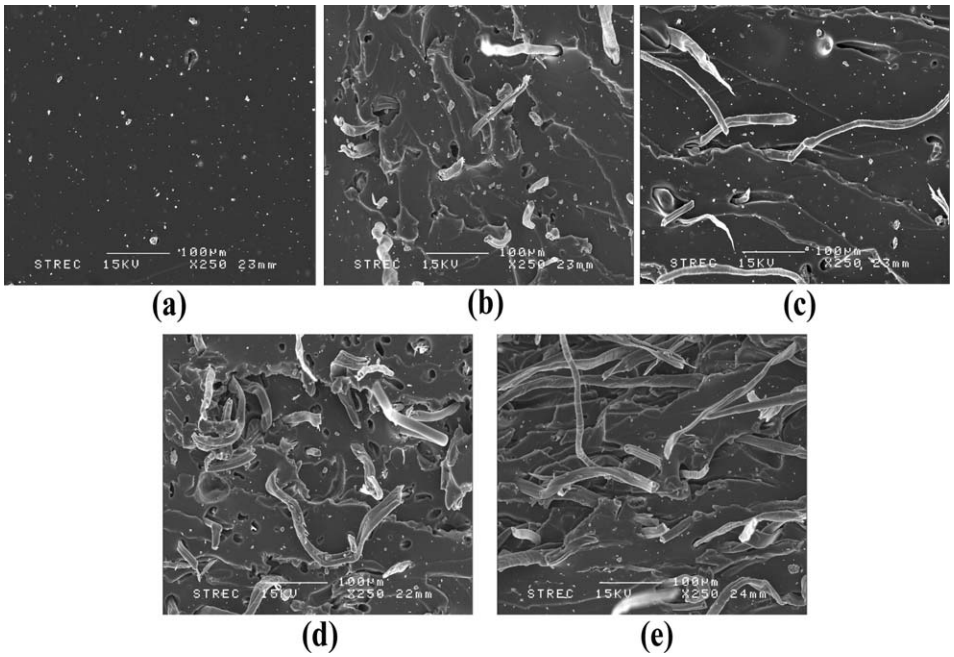

Figure 11. SEM images of HNBR composites with various loadings of cotton fiber: (a) unfilled; (b) 5 phr cotton fiber (L direction); (c) 5 phr cotton fiber (T direction); (d) 15 phr cotton fiber (L direction); and (e) 15 phr cotton fiber (T direction).

modulus (E′) caused by fiber loading is more pronounced in the rubbery region than the glassy region. This is because of the greater magnitude of molecular mobility. With increased fiber loading, rubber molecular mobility is more restricted by fiber, leading to the increase in E′. This phenomenon is known as the hydrodynamic or dilution effect. In addition, the increase in crosslink density by increasing cotton fiber loading as demonstrated earlier in Figure 6 is capable of reducing the molecular mobility to some extent. Notably, the E′ in L direction is much greater than that in T direction, agreeing well with the tensile modulus results discussed previously.

Figure 10 shows a dependence of temperature on tensile loss modulus (E″). Again, a significant change in E″ is noticeable in the rubbery region. With increasing fiber loading, the E″ increases implying increased energy loss (hysteresis loss) at fiber surfaces as a result of rubber molecular slippage on fiber surfaces. Such slippage is magnified by a poor interfacial adhesion between fiber and HNBR matrix as supported by the low BRC (see Table III). At a given fiber loading, the systems with fiber aligned in L direction exhibits greater E", due to the higher contact area between fiber surfaces and rubber matrix in parallel direction to the applied stress. It must be noted that, within the experimental tolerance, there is no significant difference in glass transition temperature (T_g), regardless of fiber loading. This supports the relatively low interfacial adhesion between fiber and HNBR matrix as discussed previously.

According to SEM images in Figure 11, the addition of 5 phr cotton fiber still gives good distribution of cotton fibers in HNBR matrix. Figure 11(b,d) exhibit fractured surfaces in the L direction in which the fibers with long L/D ratio could be observed. By contrast, the SEM images in Figure 11(c,e) show the fracture failure of composites via a pull-out mechanism which is attributed to the poor interfacial adhesion of cotton fiber and HNBR. This finding is more pronounced at high fiber loading of 15 phr as evidenced in Figure 11(d,e).

CONCLUSION

HNBR composites reinforced with cotton fiber were prepared. Degree of fiber alignment was controlled by mechanical shear stress/strain. Effects of fiber loading and alignment on mechanical properties, viscoelastic behavior, crosslink density and bound rubber content were investigated. Results reveal good dispersion and alignment of cotton fiber when the compounds are prepared at the nip width of 0.2 mm, dispersion time of 10 minutes and shear strain at arbitrary value 3.0 $\times 10^4$t. With increasing fiber loading, mechanical properties increase via the load-bearing capability of fiber in conjunction with the hysteresis loss at fiber surfaces. A control of fiber to be in longitudinal direction to the applied stress is capable of enhancing the mechanical properties drastically particularly in the rubbery region. SEM images reveal poor interfacial adhesion between HNBR matrix and cotton fiber, which is in good agreement with the bound rubber content results.

ACKNOWLEDGMENTS

The authors would like to thank the Thailand Research Fund (TRF Research Senior Scholar; RTA 5580009) for financial support throughout this work.

REFERENCES

1. Vigo, L. T.; Kinzig, B. J. Composite Applications The Role of Matrix, Fiber, and Interface; VCH Publishers: New York, **1992**.

2. Kashani, M. R. *J. Appl. Polym. Sci.* **2009**, *113*, 1355.
3. Tian, M.; Cheng, L.; Liang, W.; Zhang, L. *Macromol. Mater. Eng.* **2005**, *290*, 681.
4. Setua, D. K.; De, S. K. *J. Mater. Sci.* **1984**, *19*, 983.
5. Lopattananon, N.; Jitkalong, D.; Seadan, M. *J. Appl. Polym. Sci.* **2011**, *120*, 3242.
6. Ryu, S. R.; Lee, D. J. *KSME. Int. J.* **2001**, *15*, 35.
7. Tian, M.; Su, L.; Cai, W.; Yin, S.; Chen, Q.; Fong, H.; Zhang, L. *J. Appl. Polym. Sci.* **2011**, *120*, 1439.
8. Praveen, S.; Chattopadhyay, P. K.; Jayendran, S.; Chakraborty, B. C.; Chattopadhyay, S. *Polym. Int.* **2010**, *59*, 187.
9. Mwaikambo, L. Y.; Ansell, M. P. *J. Appl. Polym. Sci.* **2002**, *84*, 2222.
10. Dick, J. S. Rubber Technology Compounding and Testing for Performance; Hanser Publishers: Munich, **2001**.
11. Zeng, Z.; Ren, W.; Xu, C.; Lu, W.; Zhang, Y.; Zhang, Y. *J. Appl. Polym. Sci.* **2009**, *111*, 437.
12. Elappunkal, T. J.; Mathew, R.; Thomas, P. C.; Thomas, S.; Joseph, K. *J. Appl. Polym. Sci.* **2009**, *114*, 2624.
13. López-Manchado, M. A; Arroyo, M. *Polym. Composite* **2002**, *23*, 666.
14. Rajeev, R. S.; Bhowmick, A. K.; De, S. K.; Bandyopadhyay, S. *J. Appl. Polym. Sci.* **2003**, *90*, 544.
15. El-Sabbagh, S. H.; Yehia, A. A. *Egypt. J. Solids* **2007**, *30*, 157.
16. Ismail, H.; Tan, S.; Poh, B. T. *J. Elastom. Plast.* **2001**, *33*, 251.
17. Arroyo, M.; López-Manchado, M. A.; Herrero, B. *Polymer* **2003**, *44*, 2447.
18. Choi, S. S. *Polym. Test.* **2002**, *21*, 201.
19. Fröhlich, J.; Niedermeier, W.; Luginsland, H. D. *Compos. Part. A-Appl. S.* **2005**, *36*, 449.
20. Ye, X.; Tian M, Zhang, L. Q. *J. Appl. Polym. Sci.* **2012**, *124*, 927.
21. Guo, B. C.; Chen, F.; Chen, W. W.; Lei, Y. D.; Jia, D. M. *Express. Polym. Lett.* **2010**, *4*, 529.
22. Smitthipong, W.; Nardin, M.; Schultz, J.; Suchiva, K. *Int. J. Adhes. Adhes.* **2007**, *27*, 352.
23. Leblanc, J. L. *J. Appl. Polym. Sci.* **2000**, *78*, 1541.
24. Bandyopadhyay, S.; De, P. P.; Tripathy, D. K.; De, S. K. *Polymer* **1996**, *37*, 353.
25. Rattanasom, N.; Saowapark, T.; Deeprasertkul, C. *Polym. Test.* **2007**, *26*, 369.
26. Hofmann, W. Rubber Technology Handbook Germany; Hanser Publishers: Munich, **1989**.
27. Gatos, K. G.; Sawanis, N. S.; Apostolov, A. A.; Thomann, R.; Karger-Kocsis, J. *Macromol. Mater. Eng.* **2004**, *289*, 1079.